toothless tool to improve the rough model coming from the direct methods or even the model refined with single-crystal least-squares and restraints. This statement is also confirmed by other authors (Duax, 1993).

(*d*) Weak reflections are needed for a convergence towards the correct model; it is dangerous to cut off the data set at 1.5σ. It is also important to have enough reflections with respect to the number of parameters.

The authors wish to thank the E. C. ERASMUS program for bringing one of us (R. Spengler) to Amsterdam to start a collaboration on this topic.

References

BRAM, A., BRÜDERL, G., BURZLAFF, H., LANGE, J., ROTHAMMEL, J., SPENGLER, R., KARAYANNIS, M. I. & VELTSISTAS, P. G. (1994). *Acta Cryst.* C**50**, 178–180.

BRÜDERL, G., BURZLAFF, H., ROTHAMMEL, W., SPENGLER, R., ZIMMERMANN, H. & PERDIKATSIS, V. (1994). *Acta Cryst.* B**50**, 45–50.

CAGLIOTTI, G., PAOLETTI, A. B. & RICCI, F. P. (1958). *Nucl. Instrum. Methods*, **35**, 223–226.

DAVID, W. I. F. & MATTHEWMAN, J. C. (1985). *J. Appl. Cryst.* **18**, 461–466.

DUAX, W. E. (1993). Editor. IUCr Newsletter, Vol. 1, No. 2, 10.

HALL, S. R. & STEWART, J. M. (1990). Editors. *Xtal*3.0 *Reference Manual*. Univs. of Western Australia, Australia, and Maryland, USA.

HOWARD, S. A. & SNYDER, R. L. (1989). *J. Appl. Cryst.* **22**, 238–243.

JANSEN, J., PESCHAR, R. & SCHENK, H. (1992*a*). *J. Appl. Cryst.* **25**, 231–236.

JANSEN, J., PESCHAR, R. & SCHENK, H. (1992*b*). *J. Appl. Cryst.* **25**, 237–243.

JANSEN, J., PESCHAR, R. & SCHENK, H. (1993). *Z. Krist.* **206**, 33–43.

KROGH ANDERSEN, E. (1967). *Acta Cryst.* **22**, 191–196.

MAIN, P. (1985). In *Crystallographic Computing* 3, edited by G. M. SHELDRICK, C. KRÜGER & R. GODDARD, pp. 206–215. Oxford: Clarendon Press.

PESCHAR, R. (1990). In *MolEN, Molecular Structure Solution Procedures*, Vol. 3, pp. 59–82. Delft: Enraf–Nonius.

VISSER, J. W. (1969). *J. Appl. Cryst.* **2**, 89–95.

Acta Cryst. (1994). B**50**, 582–588

Structure of Oxidized Forms of Neodymium and Praseodymium (Bis)phthalocyanines

BY A. DAROVSKY AND V. KESERASHVILI*

*SUNY X*3, *National Synchrotron Light Source, BNL, Upton, NY* 11973, *USA*

R. HARLOW

Central Research and Development Department, E. I. du Pont de Nemours & Co., Experimental Station, Wilmington, DE 19880-0228, *USA*

AND I. MUTIKAINEN

Department of Chemistry, University of Helsinki, Box 6, *SF*-00014, *Finland*

(*Received* 11 *March* 1993; *accepted* 19 *April* 1994)

Abstract

The structure of the tetragonal α-phase of lanthanide derivatives of (bis)phthalocyanine $PcL^{III}Pc_{ox}$ ($Pc = [C_{32}H_{16}N_8]^{2-}$, $Pc_{ox} = [C_{32}H_{16}N_8]^{-}$, L = lanthanide) crystals is reported. The crystals of $PcNdPc_{ox}$ (I) and $PcPrPc_{ox}$ (II) crystallized on a platinum anode with (I) $a = 19.544$ (2), $c = 6.514$ (1) Å, $Z = 2$, $P4/nnc$, (II) $a = 20.066$ (7), $c = 6.463$ (2) Å, $Z = 2$, $P4/nnc$. The structure is built up from columns of equi-distantly separated sandwich-like molecules. The molecular columns are arranged in a regular square lattice, allowing the stacks to be shifted along the stack axis. The remarkable feature of this structure is the ~1:2.7 ratio of the metal-site occupancy coefficients, which is interpreted in terms of a disordered superstructure, the disorder being caused by the presence of a small amount of a triple-decker PcLPcLPc complex.

* Visiting scientist.

Introduction

The lanthanide (bis)phthalocyanine complexes have generated a lot of interest because of their high electrical conductivity (Sullivan, Dominey, Helms,

Schwartz, Ter Haar & Hatfield, 1985; Noreiga, 1988; Trojan, Hatfield, Kepler & Kirk, 1991), magnetic correlations (Petit, Holczer & Andre, 1987; Petit & Andre, 1988) and intriguing optical properties (Collin & Schiffrin, 1982). As part of the effort to understand the molecular basis of these properties, the structure of the α-phase of $PcNd^{III}Pc_{ox}$, prepared by electrochemical oxidation of the protonated compound $PcNd^{III}PcH$, was determined and refined in the non-centrosymmetric space group *P4nc* (Darovskikh, Frank-Kamenetskaja & Fundamenskii, 1986). The large variation in chemically equivalent bond lengths, the site disorder in the Nd ions and the presence of diffuse scattering suggested that this first structural model was too simple. However, the crystallographic study did reveal the basic structure, namely that the molecules stack in columnar fashion parallel to the *c* axis.

The complexity of the 'real' structure of the α-phase of the light lanthanide (bis)phthalocyanine complexes now appears to be linked with the variety of chemical species that are either present or formed during the electrochemical oxidation process. For example, the existence of both a super complex, PcLPcLPc, and a dimer of the type $PcLPc_{ox}$:$Pc_{ox}LPc$ have been postulated (M'Sadak, Roncali & Garnier, 1986; Moskalev, Shapkin & Darovskikh, 1979). In this paper, we provide evidence that the disorder and diffuse scattering in these crystals can be explained by the presence of 'triple-decker' molecules, PcLPcLPc, which interfere with ordered stacking of the $PcLPc_{ox}$ molecules.

Experimental

1,2-Dicyanobenzene, *N*,*N*-dimethylformamide, hydrazine monohydrate, praseodymium and neodymium acetate hydrates were obtained from Aldrich Chemical Company. The protonated forms of the neodymium and praseodymium derivatives of phthalocyanine were synthesized following published procedures (Kirin, Moskalev & Makashev, 1965). The crystals of $PcLPc_{ox}$ were grown electrochemically (Moskalev, Shapkin & Darovskikh, 1979). An elemental analysis of the praseodymium derivative performed by the Shwartzkopf Microanalytical Laboratory confirmed the expected Pc_2L stoichiometry of the sample.

The dark prismatic crystals of the α-phase have always been available in abundance when preparing the oxidized samples of the phthalocyanine derivatives of the light lanthanides (Pr, Nd, Eu). In addition to the sharp diffraction spots, these crystals produced diffuse lines in Laue pictures oriented perpendicular to the *c* axis, indicating the quasi-one-dimensional character of the structure in the [001] direction. An oscillation pattern (*c*-axis rotation) showed the odd layers as diffuse streaks superimposed on a few sharp reflections, while the even layers appeared as normal sharp reflections. Synchrotron radiation was used to obtain high-resolution diffraction peak profiles as a function of temperature. The ratio of the diffuse and sharp peak widths (Fig. 1) was found to be independent of temperature, indicating static positional disorder. Diffuse scattering was predominantly concentrated around reflections having indexes $l = 2n+1$, $h+k = 2n+1$. The precession photographs of *hk*0–*hk*2 layers indicated tetragonal symmetry. Crystal data are presented in Table 1.

Table 1. *Crystallographic data*

Formula	$C_{64}H_{32}N_{16}Nd$	$C_{64}H_{32}N_{16}Pr$
Molecular weight	1169	1166
Crystal system	Tetragonal	Tetragonal
a (Å)	19.544 (2)	20.066 (7)
c (Å)	6.514 (1)	6.463 (2)
V (Å^3)	2488	2602
Z	2	2
D_{calc} (g cm^{-3})	1.561	1.488
μ (cm^{-1})	11.17, Vol. 3 11.06, Vol. 4	10.0, Vol. 3 9.90, Vol. 4
Space group	*P4/nnc*	*P4/nnc*
Radiation	Mo $K\alpha$	Mo $K\alpha$
Crystal size (mm)	0.24 × 0.24 × 0.53	0.19 × 0.17 × 0.49
Scan mode	ω	ω
Scan angle (°)	2.5 + 0.35tanθ	2.0
Scan speed (° min^{-1})	4	0.75
θ limits	3/58	3/56
Octants	$h\ k\ l$	$-h\ -k\ \pm l$
No. of data measured	1063	2872
No. of refl. $F > 2\sigma_F$	930	1158
R	0.044	0.064
R_w	0.051	0.091
χ	1.92	4.1
$(\Delta/\sigma)_{max}$	3	0.3
Standard reflections	$\bar{3}71$, $\bar{1}1\bar{4}$	$\bar{4}02$, $0\bar{6}0$
Standard interval (min)	98	98
Temperature (K)	208	183
Diffractometer	CAD-4	Syntex P3F

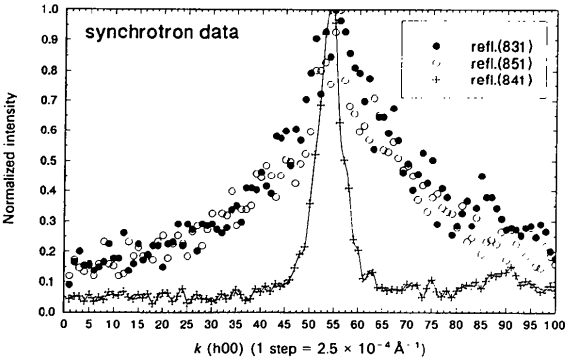

Fig. 1. Typical diffraction profiles of α-$PcPrPc_{ox}$ [$k = 2\pi(\sin\theta)/\lambda$]. The (831) and (851) reflections are part of a diffuse layer and show much broader profiles.

Weissenberg photographs taken with a long exposure time (100 h) indicated that the Laue group of the test crystals was 4/*mmm*. Systematic absences (extinction symbol *P-nc*) indicated either the centrosymmetric group *P4/mnc*, or the non-centrosymmetric one, *P4nc*. Since verification of the pyroelectric effect did not conclusively indicate that the crystals had polar character, and the least-squares refinement in the non-centrosymmetric space group did not converge well, we would ordinarily have given preference to the centrosymmetric group. However, because the expected twisted configuration of the molecular 'sandwich' typical for all metal (bis)phthalocyanines does not comply with the 4/*m* symmetry site of the metal atom in *P4/mnc*, we used a related space group *P4/nnc* for the structure determination. In this case, a few reflections of the zero-layer with $h+k=2n+1$ having intensities $2\sigma_I \le I \le 20\sigma_I$ were discarded as systematic 'extinctions'. This centrosymmetric space group places the molecule on a 422 site and eliminates the correlations that give rise to the large variations in the chemically equivalent bond distances when the structure is refined in *P4nc* (site symmetry 4).

The structure was solved by the 'heavy-atom' method, and a full-matrix least-squares refinement was performed with the *NRCVAX* program package (Gabe, Le Page, Challand & Lee, 1989). Data-collection parameters are displayed in Table 1. Orientation matrices and unit-cell parameters were obtained from 25 machine-centered reflections ($2\theta \le 25°$). Two standard reflections revealed no decay over the duration of data collection. The raw step-scan data were converted to intensities using the Lehmann–Larsen method and then corrected for Lorentz, polarization and absorption factors, the latter computed by the analytical method (Meulenaer & Tompa, 1965). Weights were based on counting statistics. Positions of H atoms were all calculated and refined with isotropic thermal parameters in an equal shift mode; all non-H atoms were refined anisotropically. The deepest hole in the final difference Fourier map was -1.59 (I), -1.15 e Å^{-3} (II), and the highest peak was 2.06 e Å^{-3} at the positions of the metal atom (I), and 2.46 e Å^{-3} at the special position (1/4, 3/4, 0) (II). Since analysis of the Patterson function revealed a statistical distribution of the metal atoms in two crystallographic positions along the *c* axis, the refinement was performed taking into account the population of those positions. There was a strong correlation ($k \simeq 0.85$) found between the occupancy coefficients and anisotropic thermal parameters U_{33} of the metals. As there are only two metal atoms in the unit cell occupying a special position (*a* or *b*) of multiplicity 2, the sum for the two possible metal sites was constrained to unity, reducing the correlation to 0.58 (I) and 0.62 (II). The coordinates and the thermal parameters of the atoms are given in Table 2.*

Table 2. *Atomic coordinates and equivalent isotropic thermal parameters of $PcNdPc_{ox}$ and $PcPrPc_{ox}$**

$B_{eq} = (1/3)\sum_i \sum_j B_{ij} a_i^* a_j^* \mathbf{a}_i.\mathbf{a}_j$.

	x	*y*	*z*	B_{eq} (Å^2)
Nd1	1/4	1/4	1/4	1.13 (1)
Nd2	1/4	1/4	3/4	3.48 (6)
N1	0.0938 (2)	0.1755 (2)	0.0036 (9)	2.6 (2)
N2	0.1548 (2)	0.2837 (2)	0.0134 (7)	2.4 (2)
C1	0.0975 (2)	0.2444 (4)	0.0040 (8)	2.4 (2)
C2	0.0366 (2)	0.2877 (2)	−0.0041 (9)	2.6 (2)
C3	−0.0331 (3)	0.2734 (4)	−0.012 (2)	3.5 (3)
C4	−0.0766 (3)	0.3289 (4)	−0.015 (1)	5.0 (1)
C5	−0.0534 (3)	0.3954 (4)	−0.018 (2)	5.0 (4)
C6	0.0162 (3)	0.4095 (3)	−0.016 (1)	3.9 (3)
C7	0.0606 (2)	0.3544 (3)	−0.007 (1)	2.6 (2)
C8	0.1354 (3)	0.3508 (3)	0.0028 (9)	2.4 (2)
Pr1	1/4	1/4	1/4	1.04 (3)
Pr2	1/4	1/4	3/4	3.6 (1)
N1	0.0958 (3)	0.1802 (3)	0.002 (1)	2.4 (3)
N2	0.1564 (3)	0.2846 (3)	0.013 (1)	2.2 (3)
C1	0.0999 (3)	0.2473 (5)	0.005 (1)	2.3 (3)
C2	0.0415 (4)	0.2912 (4)	−0.005 (1)	2.5 (3)
C3	−0.0264 (5)	0.2777 (6)	−0.003 (2)	3.6 (4)
C4	−0.0680 (5)	0.3324 (7)	−0.016 (2)	4.9 (6)
C5	−0.0432 (5)	0.3977 (6)	−0.020 (2)	5.0 (5)
C6	0.0246 (5)	0.4111 (5)	−0.013 (2)	3.7 (4)
C7	0.0659 (4)	0.3567 (4)	−0.005 (1)	2.5 (3)
C8	0.1388 (4)	0.3510 (3)	0.002 (1)	2.1 (3)

* Occupancy coefficients for the metal sites: Nd1 = 0.720 (5), Nd2 = 0.280 (5), Pr1 = 0.741 (5), Pr2 = 0.259 (5).

Discussion

The molecules of $PcNdPc_{ox}$ in the α-phase structure have 422 symmetry (Fig. 2) and pack in columns parallel to the *c* axis (Fig. 3).† The 'average' structure of the column can be described as a one-dimensional array of cofacial Pc ligands separated by the disordered lanthanide ions and rotated relative to one another by $\Psi = 39°$ (I) and 41° (II). In contrast to the 'saucer-shape' conformation of (bis)phthalocyanine molecules found in other polymorphs (Darovskikh, Tsytsenko, Frank-Kamenestskaja, Fundamenskii & Moskalev, 1984; Bennet, Broaberg & Baenziger, 1973; Darovskikh, Frank-Kamenetskaja, Fundamenskii & Golubev, 1986), the Pc ligands in the α-phase structure are essentially planar: the maximum deviation of any non-H atom from the least-squares plane drawn perpendicular to the *c* axis is only 0.06 (1) Å, while in the other polymorphs the deviation may be as large as 0.75 Å.

* Lists of structure factors and anisotropic displacement parameters have been deposited with the IUCr (Reference: CR0455). Copies may be obtained through The Managing Editor, International Union of Crystallography, 5 Abbey Square, Chester CH1 2HU, England.

† Figs. 2 and 3 were prepared by the program *SHELX/PC* (Sheldrick, 1990).

The bond lengths and bond angles (Fig. 4) for all of the polymorphs are, however, in good agreement.

The remarkable feature of the α-phase structure is the ratio of the occupancy coefficients of the metal sites, 1:2.6 (I), 1:2.8 (II). Any model of the true crystal structure must not only account for this unusual disorder, but must also explain both the inconsistency in the space-group determination and peculiarities of the diffuse scattering. Since the latter is distributed in equidistant planar sheets perpendicular to the molecular stacking direction, strict regularity along the stacking direction is indicated; the disorder must be caused by shifts in neighboring stacks. The concentration of the diffuse scattering within the odd layers around the reciprocal lattice points having indices $h+k = 2n+1$ is clear evidence of disorder between neighboring stacks. The symmetrical distribution of the diffuse scattering around those points also suggests that there are no distortions in the positions of the stacks in the direction perpendicular to the stack axis. Based on these observations, a coherent description of the disorder found in the α-phase can now be proposed. For the sake of physical clarity, we will only discuss the final results, placing the details of the calculations in the *Appendix*.

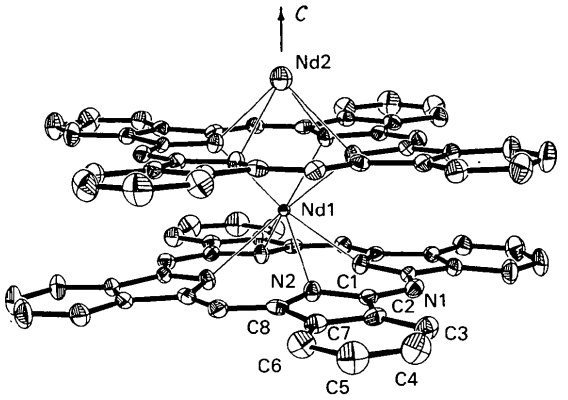

Fig. 2. A picture of the α-PcNdPc$_{ox}$ molecule. Thermal ellipsoids are drawn with 30% probability.

Let identical parallel stacks be placed at the corners of a two-dimensional square lattice (Fig. 5*a*, I) with dimensions $a'' \times a''$ ($a'' = a\sin 45°$). Depending on the character of the intermolecular interaction between the stacks, there are two possibilities for regular packing of these stacks: first, all the molecules in the stacks may be located at the same levels (Fig. 5*a*); second, the neighboring stacks may be shifted by $1/2c$ along the stack axis (Fig. 5*b*). In both models, the ratio of the metal-site occupancy coefficients (1:0 for the first and 1:1 for the second, with reference to the $a \times a \times c$ cell) is not consistent with the experimental value, which is close to 1:3. A model corresponding to the exact ratio of 1:3 is shown in Fig. 5(*c*, III), where the open circles represent stacks shifted by $1/2c$ along the stack axis. Since the true experimental ratio is not 'exact', it follows that a few other stacks (from those represented by the solid circles in Fig. 5*c*, III) are also

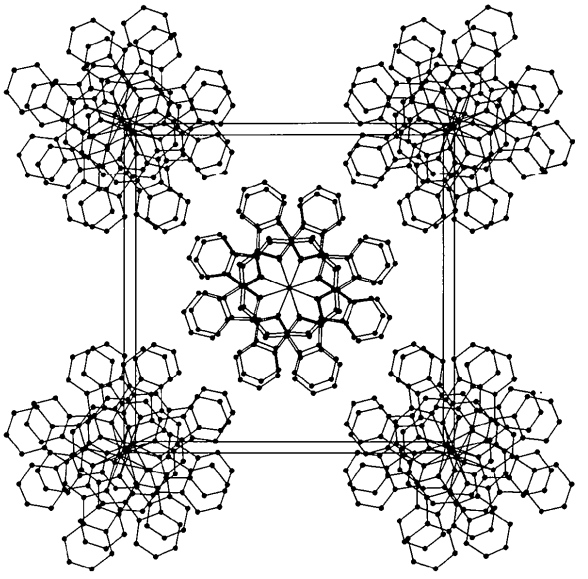

Fig. 3. Projection of the α-phase structure along the c axis. The origin is shifted to the fourfold axis for better visual impact.

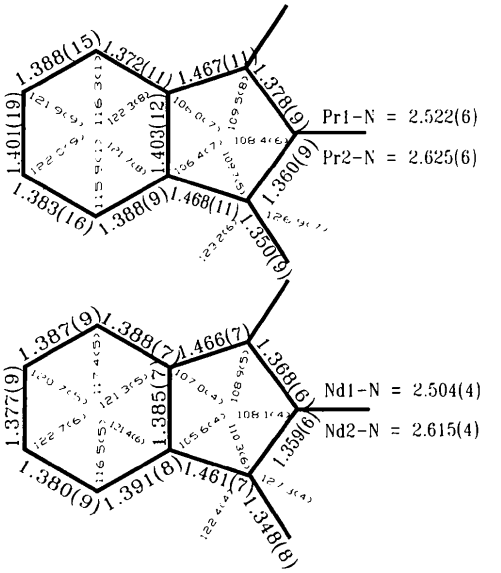

Fig. 4. Bond lengths and bond angles in α-PcNdPc$_{ox}$ and α-PcPrPc$_{ox}$.

shifted by $1/2c$ in a random fashion, breaking the translational symmetry of the supercell. The number of 'defective' cells, n, is proportional to the difference between the real and 'ideal' value of the occupancy coefficients of the equivalent metal sites. This deviation is a measure of disorder in the structure and is of the order 12 (I) and 4% (II) of the total number of supercells, N.

Suppose that only one 'defect' occurs per cell, with an equal probability of being located in the corner or on the sides of the supercell. Then there may be a total of four different cells in the structure having structure factors f_1, f_2, f_3, f_4 (*Appendix*), the structure factor of the average cell being represented by f_{av}. According to the classical diffraction theory of disordered crystals (Cowley, 1975), one can describe the total scattering from such a crystal as

$$I(\mathbf{H}) = F_{av}^2 + \Delta F^2, \qquad (1)$$

where F_{av} is a scattering amplitude of the 'average' crystal, ΔF is an amplitude of deviation from the average structure, which gives rise to the diffuse scattering, and $\mathbf{H}(h',k',l')$ is a reciprocal space vector corresponding to the cell in question. Let us consider each term of (1) individually.

$$F_{av}^2 = f_{av}^2 \sum_{i=1}^{N} \exp^{(2\pi i \mathbf{H} R_i)} \sum_{j=1}^{N} \exp^{(-2\pi i \mathbf{H} R_j)}, \qquad (2)$$

where

$$f_{av} = [(N-n)/N]f_1 + (n/4N)(f_2+f_3) + (n/2N)f_4. \qquad (3)$$

(2) describes the scattering contribution to the sharp diffraction spots corresponding to the 'average' structure based on a supercell $a' \times a'$ (Fig. 5*c*, III).

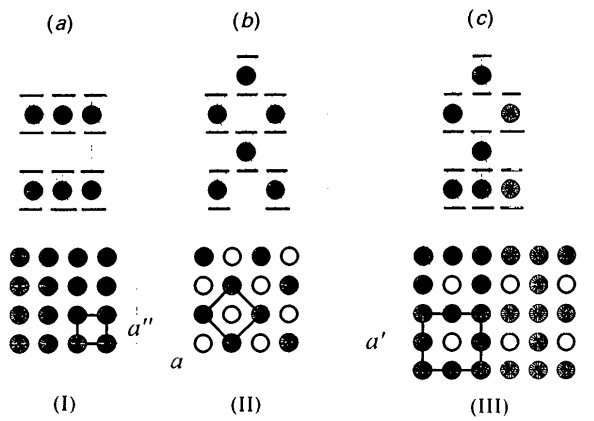

Fig. 5. Molecular stack models in the α-structure of (bis)phthalocyanines. (*a*) and (*b*) represent the arrangements of unshifted and shifted stacks, respectively; (*c*) demonstrates a molecular stack which includes a super complex molecule. (I), (II) and (III) are the projections along the stack axis. Open circles represent the stacks shifted by $1/2c$.

For the particular case of $l'=0$, a rather extended structure factor (see *Appendix*) can be reduced to

$$f_{av}^2 = 4 + 4[\cos(\pi h') + \cos(\pi k')] + 2\cos[\pi(h'-k')] + 2\cos[\pi(h'+k')]. \qquad (4)$$

One can clearly see that the strongest reflections are those having indices $(h'+k')$, with h' and k' all even. Nevertheless, the reflections with both h' and k' odd indices would have nonzero structure factors. When converted to the original cell metric by the matrix equation

$$\begin{pmatrix} h \\ k \\ l \end{pmatrix} = \begin{pmatrix} 1/2 & -1/2 & 0 \\ 1/2 & 1/2 & 0 \\ 0 & 0 & 1 \end{pmatrix} \begin{pmatrix} h' \\ k' \\ l' \end{pmatrix}, \qquad (5)$$

they give rise to the reflections having indices $h+k = 2n+1$, which explains the observed violation of the extinction rule for zero-layer reflections.

The next term describes the contribution to the diffuse scattering. This scattering, originating from the random defects, is essentially an incoherent process and, in general, has a continuous distribution in space. In our case, this term can be represented as four terms each related to the deviation of a certain type of the unit cell (f_i) from the cell corresponding to the 'average' structure (f_{av})

$$\Delta F^2 = \Delta F_1^2 + \Delta F_2^2 + \Delta F_3^2 + \Delta F_4^2. \qquad (6)$$

As n, the number of 'defects', is a small number, we need to consider only low-order terms in the expression for ΔF^2 (see *Appendix*)

$$\Delta F^2 = fs([2-2\cos(\pi l')]\{n - n^2/2N[\cos(\pi h') + \cos(\pi k')]\}). \qquad (7)$$

The first term in square brackets indicates that the diffuse scattering is located in the odd reciprocal layers only. The second term relates to the modulation of the diffuse scattering with the vectors $(\mathbf{a}')^*$ and $(\mathbf{b}')^*$, which gives rise to intensities near the reciprocal lattice points corresponding to the cell $\mathbf{a}^* \times \mathbf{b}^*$, the maxima being located at the points having both h' and k' odd or the sum of $(h+k)$ odd (for the reduced cell) in accordance with the experimental observation.

What is the nature of the 'defects' which leads to the shift of the molecular stacks by $1/2c$? It is known from the literature that the light lanthanide derivatives of phthalocyanine tend to aggregate as large sized complexes. Based on their interpretation of the optical spectra of various sublimed fractions of lanthanide (bis)phthalocyanines, M'Sadak, Roncali & Garnier (1986) assumed that the triple-decker-type complex (PcLPcLPc) is part of the synthesized prod-

uct (as well as a traces of pure phthalocyanine). The physical existence of similar complexes has been directly demonstrated by solving the structures of triple-decker complexes of (porphirinato)bis-(phthalocyaninato)dilanthanide(III) (Moussavi, De Cian, Fischer & Weiss, 1986) and dicerium(III) tris-(octaethylporphyrinate) (Buchler, De Cian, Fischer, Kihn-Botulinski, Paulus & Weiss, 1986). Having established that triple-decker complexes are possible we may expect a shift of the whole stack by $1/2c$ when such a complex is embedded into the chain during the crystal growth (Fig. 5*c*). It should be noted that the number of such super complexes is much smaller than n, the number of 'defects' responsible for the diffuse scattering; one super complex per molecular stack of the correlation length $L \simeq 1400$ Å ($L = 2\pi/\Delta k_c$) having approximately 215 (bis)phthalocyanine molecules is sufficient to produce such an effect.

Our general model based on the assumption of equal probability of 'defects' in the different stacks is sufficient to qualitatively explain the observed peculiarities of the X-ray scattering from disordered crystals of α-phase lanthanide (bis)phthalocyanines. It underestimates, however, the amplitude of the modulation wave associated with the diffuse scattering, which should be proportional to n^2 [see (7)]. It appears that the 'defects' may not be totally random but subject to interstack correlations. Further studies of the diffuse scattering will be necessary to determine the exact nature of these correlations.

We thank Professors B. O. Loopstra and H. Schenk, University of Amsterdam, The Netherlands, for stimulating critiques. The technical support of Mr W. Marshall and Mr L. Lardear is gratefully acknowledged. We also thank Dr P. Lee (ANL, USA), Mrs L. Y. Wu and Mr H. Sheu for their contribution in the early stage of data collection (room temperature). The work was partially supported by the DOE Grant No. DEFG0291ER45231.

APPENDIX

If we consider one stack of molecules separated by basic vector **c** with total length $L = N_3 c$, the scattered intensity can be written

$$I = f_s^2 = f_m^2 \sin^2 N_3 \pi \mathbf{sc} / \sin^2 \pi \mathbf{sc}, \qquad (1A)$$

where $\mathbf{s} = 2\sin\theta/\lambda = h\mathbf{a}^* + k\mathbf{b}^* + l\mathbf{c}^*$ is a diffraction vector, f_s and f_m are the scattering amplitudes of a whole stack and an individual molecule, respectively. In the case of a super cell shown in Fig. 5(*c*, III), which contains four molecular stacks, one in the center being shifted by $1/2c$, the structure factor is

$$f_1 = f_s\{1 + \exp^{(\pi i \mathbf{s}'\mathbf{a}')} + \exp^{(\pi i \mathbf{s}'\mathbf{b}')} + \exp^{[\pi i \mathbf{s}'(\mathbf{a}'+\mathbf{b}'+\mathbf{c}')]}\}$$
$$= f_s\{1 + \exp^{(\pi i h')} + \exp^{(\pi i k')} + \exp^{[\pi i(h'+k'+l')]}\}, \qquad (2A)$$

where primed symbols are related to supercell metric. In the 'defective' cell, there is one more shifted stack. It may be either one in the corner or one on the sides of the unit cell. We assume that there is an equal probability for the side and corner sites to be occupied with a shifted stack. Then we would have three types of 'defective' cells with structure factors

$$f_2 = f_s\{1 + \exp^{(\pi i h')} + \exp^{[\pi i(k'+l')]} + \exp^{[\pi i(h'+k'+l')]}\} \qquad (3A)$$

$$f_3 = f_s\{1 + \exp^{[\pi i(h'+l')]} + \exp^{(\pi i k')} + \exp^{[\pi i(h'+k'+l')]}\} \qquad (4A)$$

$$f_4 = f_s\{\exp^{(\pi i l')} + \exp^{(\pi i h')} + \exp^{(\pi i k')} + \exp^{[\pi i(h'+k'+l')]}\}. \qquad (5A)$$

The structure factor for the 'average' cell can be written as

$$f_{av} = [(N-n)/N]f_1 + (n/4N)(f_2+f_3) + (n/2N)f_4, \qquad (6A)$$

and the deviations from the 'average' cell as follows

$$\Delta f_1 = f_{av} - f_1 = (n/4N)f_2 + (n/4N)f_3 + (n/2N)f_4 - (n/N)f_1 \qquad (7A)$$

$$\Delta f_2 = f_{av} - f_2 = [(N-n)/N]f_1 + [(n/4-N)/N]f_2 + (n/4N)f_3 + (n/2N)f_4 \qquad (8A)$$

$$\Delta f_3 = f_{av} - f_3 = [(n-N)/N]f_1 + (n/4N)f_2 + [(n/4-N)/N]f_3 + (n/2N)f_4 \qquad (9A)$$

$$\Delta f_4 = f_{av} - f_4 = [(n-N)/N]f_1 + (n/4N)f_2 + (n/4N)f_3 + [(n/2-N)/N]f_4, \qquad (10A)$$

where N and n are the numbers of total and 'defective' cells, respectively.

The scattered intensity from a disordered crystal can be calculated as (Cowley, 1975)

$$I(\mathbf{H}) = F_{av}^2 + \Delta F^2 = f_{av}^2 \sum_{i=1}^{N} \exp^{(2\pi i \mathbf{H}\mathbf{R}_i)} \sum_{j=1}^{N} \exp^{(-2\pi i \mathbf{H}\mathbf{R}_j)} + \sum_{i=1}^{4} \Delta f_i^2, \qquad (11A)$$

Table 3. *Numerical coefficients of the 'average' structure factor* f^2_{av} (12)

K_1	$(16N^2 - 8Nn + 3n^2)/4N^2$
K_2	$(4N^2 - 2Nn + n^2)/2N^2$
K_3	$(8Nn - 3n^2)/4N^2$
K_4	$(8N^2 - n^2)/4N^2$
K_5	n/N
K_6	$(8N^2 - 4Nn + n^2)/4N^2$
K_7	$(4Nn - n^2)/4N^2$
K_8	$(4Nn - n^2)/8N^2$
K_9	$(2N - n)/N$

where F_{av} is a scattering amplitude of the 'average' crystal, ΔF is an amplitude of deviation from the averaged structure which gives rise to the diffuse scattering, $\mathbf{R}(x,y,z)$ and $\mathbf{H}(h',k',l')$ are the direct and reciprocal space vectors, respectively. To calculate the intensity properly one should remember that structure factors [(2A)–(5A)] are the complex numbers, so that $f^2_{av} = f_{av} \times f^*_{av}$ and $\Delta f_i^2 = \Delta f_i x \Delta f_i^*$, where f^*_{av} and Δf_i^* are the complex conjugates. The squared structure factor for the 'average' crystal would then have a rather complicated form which can be written as

$$\begin{aligned} f^2_{av} = {} & K_1 + K_2(\cos\pi h' + \cos\pi k') + K_3\cos\pi l' \\ & + K_4[\cos\pi(h' + l') + \cos\pi(k' + l')] \\ & + K_5\cos\pi(h' + k') + K_6\cos\pi(h' - k') \\ & + K_7[\cos\pi(h' - l') + \cos\pi(k' - l')] \\ & + K_8[\cos\pi(h' - k' + l') + \cos\pi(k' - h' + l')] \\ & + K_9\cos\pi(h' + k' + l'), \end{aligned} \tag{12A}$$

where coefficients are presented in Table 3.

The diffuse scattering terms Δf_i^2 will have the following forms, respectively

$$\begin{aligned} \Delta f_1^2 = {} & f_s^2/N^2\{(2 - 2\cos\pi l')[3n^2/4 + (n^2/4)(\cos\pi h' \\ & + \cos\pi k') + (n^2/8)\cos\pi(h' - k')]\} \end{aligned} \tag{13A}$$

$$\begin{aligned} \Delta f_2^2 = {} & f_s^2/N^2\{(2 - 2\cos\pi l')[(N^2 - n/4)^2 + (n^2/4)] \\ & - (2 - 2\cos\pi l')n(N - n/4)\cos\pi h' \\ & + n^2/4[\cos\pi k' - \cos\pi(k' - l')] \\ & - n^2/2(N - n/4)[\cos\pi(h' - k') \\ & - \cos\pi(h' - k' + l')] + n^2/16\} \end{aligned} \tag{14A}$$

$$\begin{aligned} \Delta f_3^2 = {} & f_s^2/N^2\{(2 - 2\cos\pi l')[(N^2 - n/4)^2 + (n^2/4)] \\ & - (2 - 2\cos\pi l')n(N - n/4)\cos\pi k' \\ & + n^2/4[\cos\pi h' - \cos\pi(h' - l')] \\ & - n^2/2(N - n/4)[\cos\pi(h' - k') \\ & - \cos\pi(k' - h' + l')] + n^2/16\} \end{aligned} \tag{15A}$$

$$\begin{aligned} \Delta f_4^2 = {} & f_s^2/N^2[(2 - 2\cos\pi l')(N^2 - Nn + 3n^2/8) \\ & - n/2(N - n/2)(\cos\pi h' + \cos\pi k') \\ & + (n^2/8)\cos\pi(h' - k')] \end{aligned} \tag{16A}$$

$$\begin{aligned} \Delta F^2 = {} & \Delta F_1^2 + \Delta F_2^2 + \Delta F_3^2 + \Delta F_4^2 \\ = {} & (N - n)\Delta f_1^2 + n/4\Delta f_2^2 + n/4\Delta f_3^2 + n/2\Delta f_4^2 \end{aligned} \tag{17A}$$

The total intensity of the diffuse scattering can then be calculated from the equation

$$\begin{aligned} \Delta F^2 = {} & f_s^2/N^2\{(2 - 2\cos\pi l')[N^2 n - n^2/4(N + n/4) \\ & \times (\cos\pi h' + \cos\pi k') - n^3/16\cos\pi(h' - k')] \\ & + n^3/16\cos\pi(h') + n^3/16\cos\pi(k') \\ & + n^3/16\cos\pi(h' - l') + n^3/16\cos\pi(k' - l')\}. \end{aligned}$$

References

BENNET, W. E., BROABERG, D. E. & BAENZIGER, N. C. (1973). *Inorg. Chem.* **12**, 930–936.

BUCHLER, J. W., DE CIAN, A., FISCHER, J., KIHN-BOTULINSKI, M., PAULUS, H. & WEISS, R. (1986). *J. Am. Chem. Soc.* **108**, 3652–3659.

COLLIN, G. C. S. & SCHIFFRIN, D. J. (1982). *J. Electroanal. Chem. Interfacial Electrochem.* **139**, 335–369.

COWLEY, J. M. (1975). *Diffraction Physics*. Amsterdam: North-Holland.

DAROVSKIKH, A. N., FRANK-KAMENETSKAJA, O. V. & FUNDAMENSKII, V. S. (1986). *Sov. Phys. Crystallogr.* **31**(5), 534–537.

DAROVSKIKH, A. N., FRANK-KAMENETSKAJA, O. V., FUNDAMENSKII, V. S. & GOLUBEV, A. M. (1986). *Sov. Phys. Crystallogr.* **31**(5), 165–168.

DAROVSKIKH, A. N., TSYTSENKO, A. K., FRANK-KAMENETSKAJA, O. V., FUNDAMENSKII, V. S. & MOSKALEV, P. N. (1984). *Sov. Phys. Crystallogr.* **29**(3), 273–276.

GABE, E. J., LE PAGE, Y., CHALLAND, G. P. & LEE, F. L. (1989). *J. Appl. Cryst.* **22**, 384–387.

KIRIN, I. S., MOSKALEV, P. N. & MAKASHEV, Y. A. (1965). *Russ. J. Inorg. Chem.* **10**, 1951–1953.

MEULENAER, J. DE & TOMPA, H. (1965). *Acta Cryst.* **19**, 1014–1018.

MOSKALEV, P. N., SHAPKIN, G. N. & DAROVSKIKH, A. N. (1979). *Russ. J. Inorg. Chem.* **24**(2), 188–192.

MOUSSAVI, M., DE CIAN, A., FISCHER, J. & WEISS, R. (1986). *Inorg. Chem.* **25**(13), 2107–2108.

M'SADAK, M., RONCALI, J. & GARNIER, F. (1986). *J. Chim. Phys. Phys. Chim. Biol.* **83**, 211–216.

NOREIGA, J. P. (1988). Dissertation. Univ. of North Carolina, USA.

PETIT, P. & ANDRE, J. J. (1988). *J. Phys. (France)*, **49**, 2059–2063.

PETIT, P., HOLCZER, K. & ANDRE, J. J. (1987). *J. Phys.* **48**, 1363–1367.

SHELDRICK, G. M. (1990). *SHELX/PC*. Revision 4.2. Siemens Analytical X-Ray Instrument, Inc., Madison, Wisconsin, USA.

SULLIVAN, B. W., DOMINEY, R. N., HELMS, J. H., SCHWARTZ, M., TER HAAR, L. W. & HATFIELD, W. E. (1985). *Mol. Cryst. Liq. Cryst.* **120**, 433–437.

TROJAN, K. L., HATFIELD, W. E., KEPLER, K. D. & KIRK, M. L. (1991). *J. Appl. Phys.* **69**(8), 6007–6009.